INSIST Vol. 4 No. 2, October 2019 (221–225)
http://insist.unila.ac.id/
DOI:10.23960/ins.v4i2.221
eSSN: 2502-8588
Received: 19/05/2019
Accepted: 02/08/2019
Published online: 20/10/2019

Simulation of Cement Mill to Predict and Mitigate the Over-Heat Phenomenon: an Approach to Optimize the Energy Consumption in Cement Industry

Himawan Tri Bayu Murti Petrus[1, 2 *], Jonas Kristanto [1], Kevin Cleary Wanta[3], Agus Prasetya [1,2]

Abstract—being one of the most energy-intensive industries, cement industry requires to evaluate the energy efficiency of their operating units, one of them is cement mill. Functioning as a mixing unit of several materials, i.e., clinker, limestone, gypsum, and trass with their initial heat and propensity of heat generation during milling, over-heat in the cement mill occurs frequently. It should be avoided in order to establish efficiency. Therefore, a mathematical model was generated in this study to predict and to mitigate this overheat phenomenon. This cement mill mathematical model has been generated using mass and energy balances. The output of the model is temperature profile versus residence time with targeted water content of the product that the optimum residence time can be calculated. Based on the temperature profile with a targeted water content of the product, it can be concluded that the optimum operating condition of the cement mill lies in the range of 5 to 30 seconds of materials residence time in the cement mill.

Keywords—Cement mill, Mass balance, Energy balance, Residence time

I. INTRODUCTION

In the industrial sector, the energy consumption is one factor needing tremendous attention. It happens because this energy factor is particularly related to economic and environmental problems. Economically, high energy consumption will increase production cost, so it is difficult for the company to achieve a high profit. In addition, the consumption of high energy, using electricity or heat, harms the environment, precisely the problem of carbon dioxide (CO_2) emissions [1]. As a result, energy efficiency has to be done.

The cement industry is an industry that is classified as an energy-intensive industry [2]. This industry requires much energy in nearly all production processes. In the cement industry, energy consumption has started from limestone mining, transportation, crushing, milling, calcination, pyro-processing, cooling to grinding, as shown in Figure 1 [3]. In [4] stated that the calcination and drying stages, such as a kiln, require high thermal energy. Meanwhile, other stages or production equipment, such as milling, fan, etc. no less electric energy.

[1] Department of Chemical Engineering (Sustainable Mineral Processing Research Group), Faculty of Engineering, Universitas Gadjah Mada, Jl. Grafika 2 Yogyakarta, 55281, Indonesia
[2] Unconventional Georesources Research Center, Faculty of Engineering, Universitas Gadjah Mada, Jl. Grafika 2 Yogyakarta, 55281, Indonesia
[3] Department of Chemical Engineering, Faculty of Industrial Technology, Parahyangan Catholic University, Jl. Ciumbuleuit 94, Bandung, 40141, Indonesia
[*]Corresponding author: bayupetrus@ugm.ac.id

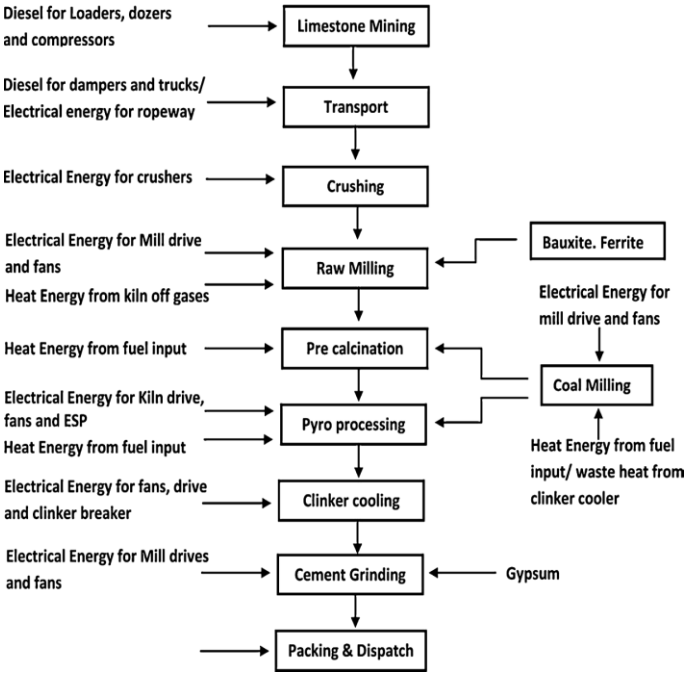

Fig. 1. Energy flow in the cement industry [3]

The high energy consumption cause utility cost, especially energy cost, increase significantly. The cost incurred for covering this energy can reach 40% of the total production costs [6]. Therefore, the cement industry needs an effort to make efficiency in energy consumption. This action of increasing energy use efficiency in energy-intensive industries is proven to substantially contribute to improving their economic and environmental attractiveness [6–7].

One effort to streamline energy consumption is in identifying and evaluate the process that consumes the most energy. One of the most energy-intensive stages of the cement production is at the cement grinding/milling or the clinker and other materials such as limestone size reduction stage [8]. In this study, we are focused on one problem that can occur in the cement mill unit due to operating temperature conditions. The cement enters this unit in hot conditions because it comes out of the kiln at high temperatures. On the other side, the milling process also has to be done at high temperatures to eliminate the water from the cement product. To balance the energy, the unit needs additional steam. However, the addition of unregulated steam will cause an overheating condition. When that condition occurs, the process has to be shut down. Consequently, the cement production will be hampered and the energy consumption will increase due to the start-up process of the mill unit.

INSIST Vol. 4 No. 2, October 2019 (221–225)
http://insist.unila.ac.id/
DOI:10.23960/ins.v4i2.221

Received: 19/05/2019
Accepted: 02/08/2019
Published online: 20/10/2019

The main focus of this study is to develop a simple mathematical model of the process inside of the cement mill, finding the mass transfer parameters, developing the water content and temperature profile of materials inside of the cement mill. The result of this study is a range of optimal operational condition of the cement mill.

II. METHODOLOGY

A. Data Collection

We conducted a study in Plant 6-11 of PT. Indocement Tunggal Prakasa Tbk. which the cement grinding section called as the cement mill unit. The cement mill's unit main equipment is the ball mill or called merely as the cement mill.

Data of the cement mill input, output, and process parameters were received from the Engineering Team of Plant 6-11 of PT. Indocement Tunggal Prakasa Tbk. Other parameters such as material heat capacity, heat conductivity, density, etc. were compiled from reliable references [9–10]. Figure 2 shows the cement mill apparatus that is generally used in cement industries with length of about 14 meters. While the characteristic of the solid materials ground in the cement mill is shown in table 1. As for the heat capacity of each component in this cement mill system tabulated in table 2.

Table 1. Characteristics of the milled solid materials

Materials	% mass	Mointure content (db)	Temperature (°C)
Clinker	59.6	0	120
Limestone	34	2.56	26
Gypsum	2.4	4.84	26
Trass	4	15.22	26

Table 2. Heat capacity of each component

Component	Heat capacity (cal/g/°C)
Clinker	0.186
Limestone	0.217
Gypsum	0.259
Water (liquid)	8.712+1250e-6*T–0.18e-6*T^2 (cp/R)
Water (vapor)	3.47+0.00145*T+0.121*T^-2 (cp/R)
Water vaporization (latent heat)	2256.9 J/g (at 100°C)

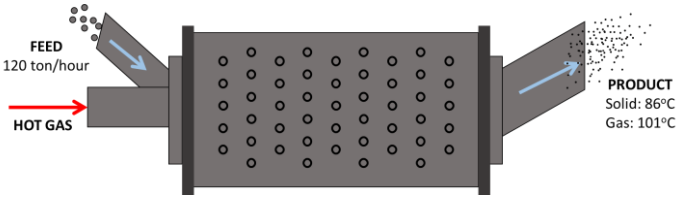

Fig. 2. Cement Mill Apparatus

B. Mass and Heat Transfer Model

To provide a logical result from the limited data we had, we made some assumptions to ease our calculations. The first assumption assumes that the particle shape of these materials is spherical and averaged at 1.2725 mm. Although it is obvious that size reduction is one of the most important duties of the ball mill, taking the average number of sizes of these materials is the easiest way to obtain a relevant result. Secondly, the transfer of water vapor only occurs between the solid-state material (clinker, limestone, gypsum, and trass) and air. Mass transfer between the solid-state material may occur due to contact between them. However, these particle sizes are too small (average at 1.2725 mm) which may result in an insignificant amount of mass transferred between them. The third assumption of this evaluation assumes that the air surrounding the cement mill had a velocity of 3 m/s. The fourth assumption assumes that the water diffusivity and the water mass transfer Henry coefficient between these 4 materials and air are the same. This last assumption is made because the water content of the product does not specify to each material, but only the bulk water content. Moreover, the last assumption assumes that the steel ball has a constant temperature.

Data from the source we have were fitted into mass and heat transfer model to find the effective diffusivity and Henry Isotherm Constant of materials. The following model applies for water in each solid materials mass balance (equation 1).

$$\frac{\partial C_i}{\partial t} = D_e.\frac{\partial^2 C_i}{\partial r^2} + \frac{2.D_e}{r}.\frac{\partial C_i}{\partial r} \qquad (1)$$

with C_i for water concentration in each solid material, D_e for effective diffusivity of water in each solid material, r for the radius of solid materials, and t for time. Furthermore, the mass balance of water in the hot gas follows equation 2.

$$\frac{dC_{HG}}{dt} = \frac{v}{F}.\sum_{i=1}^{4}\left(k_m.4\pi.R_i^2.\rho_{s_i}.\left(C_i - \frac{C_{HG}}{H}\right).\frac{Nb_i}{L}\right) \qquad (2)$$

with C_{HG} for water concentration in the hot gas, v for hot gas velocity, F for hot gas mass flow rate, k_m for water mass transfer coefficient, R_i for the radius of solid materials, ρ_{s_i} for the density of solid materials, H for Henry Isotherm Constant, Nb_i for a total particle of material, and L for the length of the cement mill. These equations obviously need initial and boundary condition to be solved. These following equations (3, 4, 5, and 6) are the suitable initial and boundary condition:

$$C_i(r,0) = C_{i_0} \qquad (3)$$

$$-D_e.4\pi.r^2.\rho_{s_i}.\left.\frac{\partial C_i}{\partial r}\right|_{r=0} = 0 \qquad (4)$$

$$-D_e.4\pi.R^2.\rho_s.\left.\frac{\partial C_i}{\partial r}\right|_{r=R_i} = k_m.4\pi.R_i^2.\rho_{s_i}.\left(C_i - \frac{C_{HG}}{H}\right) \qquad (5)$$

$$C_{HG}|_{z=0} = C_{HG_0} \qquad (6)$$

The first three equations (3, 4, and 5) above applied for the mass balance of water in solid materials. The equation 3 is the initial condition where solid materials have their initial water content when they enter the cement mill. The equation 4 applies at the center of each material where the water content is always at minimum for clinker and always at maximum for

INSIST Vol. 4 No. 2, October 2019 (221–225)
http://insist.unila.ac.id/
DOI:10.23960/ins.v4i2.221

Received: 19/05/2019
Accepted: 02/08/2019
Published online: 20/10/2019

gypsum, limestone, and TRASS. The equation 5 applies at the radius of solid materials where the mass transfer of water is equal to the convective mass transfer from solid materials to hot gas. Moreover, the equation 6 is the initial condition of the hot gas when it enters the cement mill.

To support the mass balance, we also integrated an equation to find the correlation between the mass transfer coefficient and the effective diffusivity for solid particles suspended in the agitated vessel as shown in the equation 7. [10]

$$Sh = 2 + 0{,}6.Re^{\frac{1}{2}}.Sc^{\frac{1}{3}} \tag{7}$$

with Sh for Sherwood Number $\left(\frac{k_m.2.r}{D_e}\right)$, Re for Reynold Number $\left(\frac{\rho.v.2.r}{\mu}\right)$, Sc for Schmidt Number $\left(\frac{\mu}{\rho.D_e}\right)$, μ for hot gas viscosity, and ρ for hot gas viscosity.

The next equation that applies to this study is the heat balance equations. The equation 8 applies for solid materials:

$$\frac{\partial T_i}{\partial t} = \left\{ \begin{array}{c} D_e.\frac{cp_w}{(cp_s + cp_w.C_i)}.T_i.\frac{\partial^2 C_i}{\partial r^2} + D_e.\frac{2}{r}.\frac{cp_w}{(cp_s + cp_w.C_i)}.T_i.\frac{\partial C_i}{\partial r} + \\ \frac{k}{\rho_{s_i}.(cp_s + cp_w.C_i)}.\frac{\partial^2 T_i}{\partial r^2} + \frac{2.k}{r.\rho_{s_i}.(cp_s + cp_w.C_i)}.\frac{\partial T_i}{\partial r} - \\ \frac{cp_w}{(cp_s + cp_w.C_i)}.T_i.\frac{\partial C_i}{\partial t} \end{array} \right\} \tag{8}$$

with T_i for solid materials temperature, cp_w for water heat capacity, cp_s for solid materials, heat capacity, and k for solid materials heat conductivity. Furthermore, the heat balance of hot gas follows the equation 9:

$$\frac{dT_{HG}}{dt} = \frac{\left[\begin{array}{c} \Sigma_{i=1}^{4} \left\{ \begin{array}{c} h_i.4\pi.R_i^2.(T_i - T_{HG}).\frac{Nb_{i_{total}}}{L} + \\ k.4\pi.R_i^2.\left(C_i - \frac{C_{HG}}{H_i}\right).cp_{water\ vapor}.\rho_{s_i}.T_{air}.\frac{Nb_{i_{total}}}{L} \end{array} \right\} - \\ \frac{F.cp_{water\ vapor}.T_{HG}}{v}.\frac{dC_{HG}}{dt} - \\ \frac{UA}{A}.\pi.d_{CM}.(T_{HG} - T_{air}) - \\ h.\frac{Nb_{SB_{total}}}{L}.4\pi.R_{SB}^2.(T_{HG} - T_{SB}) \end{array} \right]}{\frac{F.(cp_{air} + C_{air}.cp_{water\ vapor})}{v}} \tag{9}$$

with T_{HG} for hot gas temperature, T_{SB} for steel ball temperature, T_{air} for air temperature, $cp_{water\ vapor}$ for water vapor heat capacity, cp_{air} for air heat capacity, and R_{SB} for steel ball radius, h for steel ball-hot gas heat convection coefficient, d_{CM} for cement mill diameter, and UA for area-specific heat transfer coefficient of cement mill to air. Same as the mass balance equations, these following equations (10, 11, 12, and 13) are the suitable initial and boundary conditions:

$$T(r, 0) = T_0 \tag{10}$$

$$-k.4\pi.r^2.\left.\frac{\partial T}{\partial r}\right|_{r=0} = 0 \tag{11}$$

$$-k.4\pi.R^2.\left.\frac{\partial T}{\partial r}\right|_{r=R} = h.4\pi.R^2.(T - T_{udara}) \tag{12}$$

$$T_{HG}|_{z=0} = T_{HG\,0} \tag{13}$$

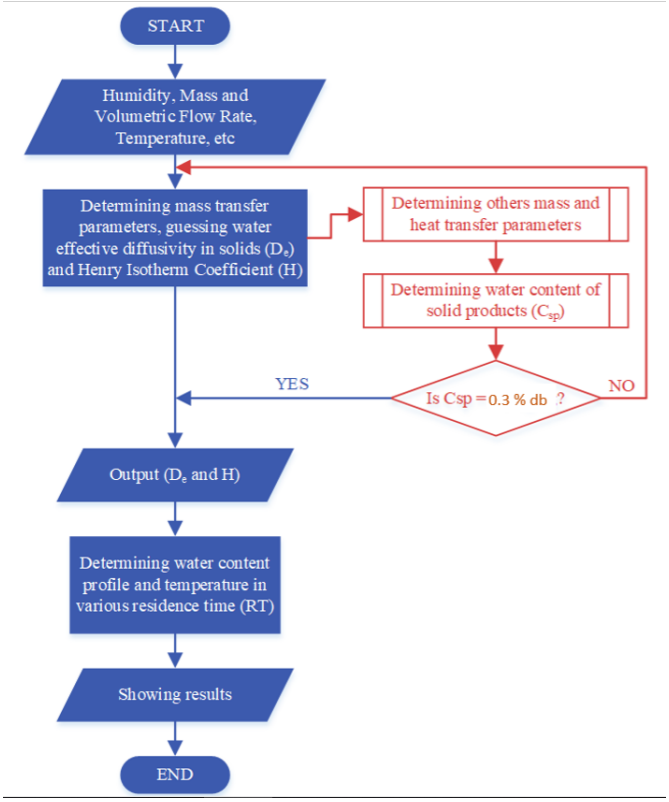

Fig. 3. Flowchart of Data Analysis Algorithm

The first three equations (10, 11, and 12) above applied for the heat balance of solid materials. The equation 10 is the initial condition where solid materials have their initial temperature when they enter the cement mill. The equation 11 applies at the center of each material where the water content is always at maximum for clinker and always at minimum for gypsum, limestone, and TRASS. The equation 12 applies at the radius of solid materials where the heat transfer of there is equal to the convective heat transfer from solid materials to hot gas. And the equation 13 is the initial condition of the hot gas when it enters the cement mill.

To support the heat balance, we also integrated equations to find the steel ball-hot gas heat convection coefficient, the convective heat transfer coefficient for gas in pipe-shaped form, and the convective heat transfer coefficient from pipe-shaped from to gas. The equations (14, 15, and 16) are [11]:

$$Nu = 0{,}37.Re^{0{,}6} \tag{14}$$

$$Nu = 0{,}027.Re^{0{,}8}.Pr^{\frac{1}{3}} \tag{15}$$

$$Nu = 0{,}332.Re^{0{,}5}.Pr^{\frac{1}{3}} \tag{16}$$

with Nu for Nusselt Number $\left(\frac{h.2.r}{k}\right)$ and Pr for Prandtl Number $\left(\frac{cp.\mu}{k}\right)$.

INSIST Vol. 4 No. 2, October 2019 (221–225)
http://insist.unila.ac.id/
DOI:10.23960/ins.v4i2.221

Received: 19/05/2019
Accepted: 02/08/2019
Published online: 20/10/2019

C. Data analysis to find mass transfer parameters

With the combination of mass and heat transfer equations, we search for the value of solid materials effective diffusivity and Henry Isotherm Constant. Each of the equations was not linearized but directly evaluated parameters-by-parameters in MATLAB® using the fminsearch function to minimize the sum square of error (SSE) of the simulated data resulted from the guessed parameters and the experimental data as shown in equation 17:

$$SSE = \left(C_{solid\ product_{calculated}}\Big|_{z=L} - C_{solid\ product_{observed}}\Big|_{z=L}\right)^2 \quad (17)$$

where $C_{solid_{calculated}}$ is the water concentration in the solid product as in MATLAB® simulation and $C_{solid_{observed}}$ is the observed water concentration in solid product.

D. Algorithm

To summarize the process of this study analysis, the algorithm of this study is shown in the following Figure 3.

III. Results And Discussion

The simulation of this mass and heat transfer evaluation in the ball mill had been done in MATLAB by predicting the appropriate water diffusivity and the water mass transfer Henry Isotherm Coefficient between 4 (four) solid materials and air to obtain the right product water content of 0.3%. The profile of water content in each solid, bulk water content in solid, and water content in hot gas generated by the simulation is displayed in Figure 4 and 5 respectively.

We can see in Figure 4 that the water content in clinker increases along with the length of cement mill and dereases for other 3 (three) solid materials, i.e. limestone, gypsum, and trass. This result is logical and verifies the mass transfer model is legitimate. In Figure 5, the bulk water content in solid materials falls simultaneously with the increase of the water content in hot gas. This also verifies the result at where the product of the cement mill possesses lower water content in comparison to that of the solid materials entering the cement mill.

In Figure 6, we can see that at the beginning, there is a significant increase in the temperature of solid-state material and a decrease in hot gas temperature. This heat exchange caused by the difference between materials temperature and the vaporization and condensation of the water content from each material. In the latter stage, the temperature of these materials decreases due to the heat transfer from these materials to the surrounding air of the cement mill. After we have the result of the correct mass and heat transfer models and parameters, we can simulate any kind of scenario. In this study, we conducted some scenarios for various residence time (RT) of hot gas and solid materials which results are displayed in Figure 7.

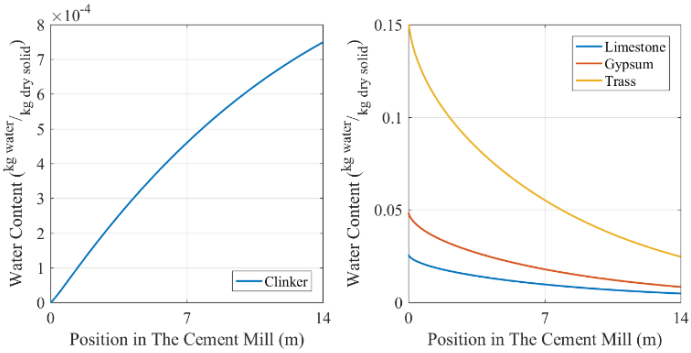

Fig. 4. Water content in specified solid materials along the cement mill

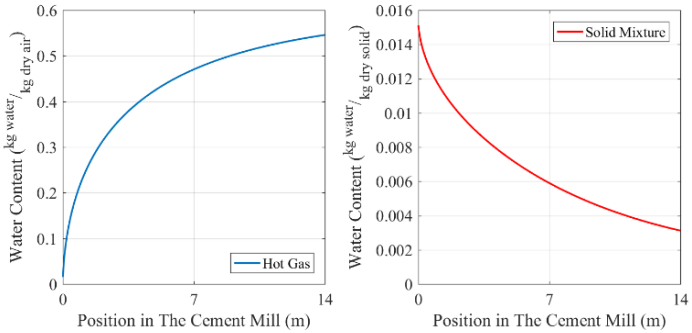

Fig 5. Bulk water content in solid materials and hot gas along the cement mill

From the data in Figure 7, we can see that lower RT will result much humid product even though this condition needs higher hot gas flow rate. This phenomenon caused by the contact time between solids and gas is too short and the increase of hot gas becomes meaningless. Although lower hot gas flow rate or higher residence time will cause lower product water content, much longer residence time will decrease cement mill efficiency as seen in simulated data with a residence time of 30 and 60 seconds at where the water content reaches the plateau before the end of cement mill length. Subsequently, an optimum condition for the operational condition of the cement mill lies between 5 and 30 seconds of residence time. To add another factor to search for the optimum operational condition of the cement mill, the temperature profile of hot gas is shown in Figure 8.

Hot gas temperature is able to represent the maximum temperature in the cement mill, as shown in Figure 6 at where the temperature of hot gas always higher than other materials. Therefore, in Figure 8 the temperature of hot gas in various residence time represents the highest temperature in the cement mill. This information is beneficial to avoid the overheating of the cement mill that will cause unit shut down and liability. At the end, we can see that the profile of water content and temperature in the cement mill for various scenarios of residence time. This information gave us a clue for the optimum condition of the cement mill operation which lies between 5 to 30 seconds of residence time as shown in Figure 7.

Received: 19/05/2019
Accepted: 02/08/2019
Published online: 20/10/2019

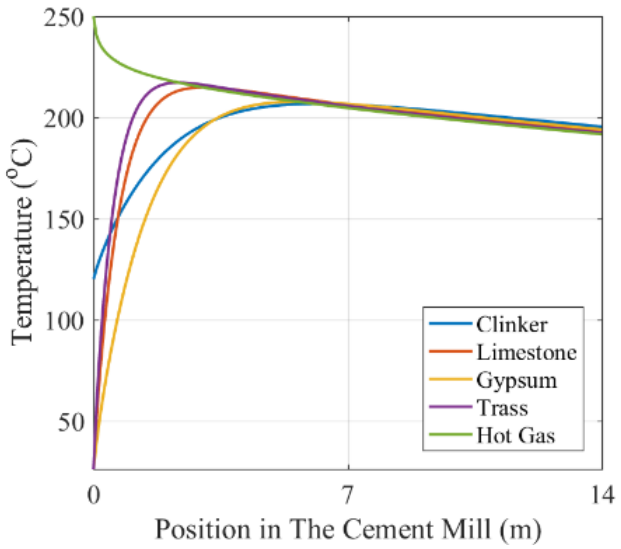

Fig. 6. The temperature of specified materials and hot gas along the cement mill

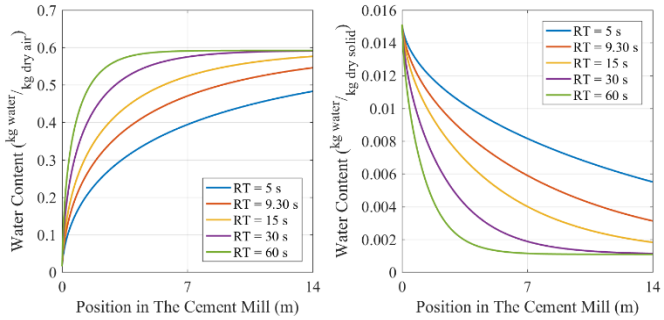

Fig. 7. Water content in solid materials and hot gas along the cement mill for some scenarios of residence time (RT)

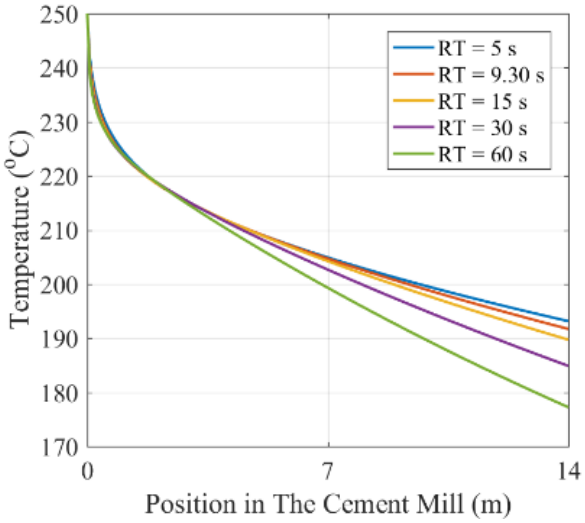

Fig. 8. Temperature Profile of Hot Gas in Cement Mill for A Few Scenarios of Residence Time (RT)

To determine the best result, more data like the correlation of residence time with energy, cost, and the correlation of product temperature and water content with the unit after the cement mill are needed.

IV. Conclusion

This study concludes that the temperature of hot gas in the cement mill able to represent the maximum temperature of the material mixture inside of the cement mill and the most optimum operating condition of the cement mill lies between 5 and 30 seconds of materials residence time inside of the cement mill.

Acknowledgment

The authors would like to thank PT. Indocement Tunggal Prakasa Tbk. for their support of this study in the form of the data supplied and the information of their production scheme in Plant 6-11 PT. Indocement Tunggal Prakasa Tbk., Citereup, Bogor, West Java.

References

[1] Worrell, E., Price, L., Martin, N., Hendriks, C., and Media, L., O., 2001, Carbon Dioxide Emissions from the Global Cement Industry, Annu. Rev. Energy Environ., 26, 303 – 329.

[2] U.S. Energy Information Administration, 2016, Chapter 7, Industrial sector energy consumption, International Energy Outlook 2016, https://www.eia.gov/outlooks/ieo/pdf/industrial.pdf

[3] Madlool, N.A., Saidur, R., Hossain, M.S., and Rahim, N.A., 2011, A critical review on energy use and savings in the cement industries, Renewable and Sustainable Energy Reviews, 15, 2042 – 2060.

[4] Wang, J., Dai, Y., Gao, L., 2009, Exergy analyses and parametric optimizations for different cogeneration power plants in cement industry, Applied Energy, 86, 941 – 948.

[5] PT. Indocement Tunggal Prakasa Tbk. (2018) 2018 Annual Report of PT. Indocement Tunggal Prakasa Tbk. Available at: papers://d3978ab5-8702-4bf9-be6f-7c3f6904d049/Paper/p5081.

[6] Aplak, H. S. and Sogut, M. Z. (2013) 'Game theory approach in decisional process of energy management for industrial sector', Energy Conversion and Management. Elsevier Ltd, 74, pp. 70–80. doi: 10.1016/j.enconman.2013.03.027.

[7] Subic, A. et al. (2013) 'Performance analysis of the capability assessment tool for sustainable manufacturing', Sustainability (Switzerland), 5(8), pp. 3543–3561. doi: 10.3390/su5083543.

[8] Hoenig, V. et al. (2013) 'Energy efficiency in cement production; part 1', Cement International, 11(4), pp. 46–65. Available at: https://www.scopus.com/inward/record.uri?eid=2-s2.0-84885574999&partnerID=40&md5=cd3f8c87a4ffc451360c76ac6df947dd.

[9] Smith, J. M., Van Ness, H. C. and Abbott, M. M. (2001) Introduction to Chemical Engineering Thermodynamics. 6th edn. New York: McGraw-Hill.

[10] Green, W. G. and Perry, H. R. (2013) Perry's Chemical Engineers' Handbook, Journal of Chemical Information and Modeling. doi: 10.1017/CBO9781107415324.004.

[11] Holman, J. P. (2009) 'Heat Transfer', p. 752. doi: 10.1115/1.3246887.